Nature of the electronic states in the layered perovskite noncuprate superconductor Sr_2RuO_4

M. Schmidt, T. R. Cummins, M. Bürk, D. H. Lu, N. Nücker, and S. Schuppler
Forschungszentrum Karlsruhe, Institut für Nukleare Festkörperphysik, Postfach 3640, D-76021 Karlsruhe, Germany

F. Lichtenberg
VARTA Batterie AG, R&D Center, 65779 Kelkheim, Germany

(Received 5 March 1996)

Near-edge x-ray-absorption and photoemission spectra of the noncuprate superconductor Sr_2RuO_4 are presented. Holes close to the Fermi level are determined by Ru $4d_{xy}$, $4d_{xz}$, and $4d_{yz}$ antibonding states. The density of the occupied states at the Fermi level derived from photoemission is higher than in the cuprates and these states have predominantly Ru 4*d* character. Angle-resolved photoemission yields a width of the occupied part of the conduction bands that is reduced by a factor of 2 in comparison to band-structure calculations. The importance of electron correlations is also evident in the appearance of screened final states in the Ru 3*d* core-level spectrum. [S0163-1829(96)51422-0]

In the past decade, following the discovery of the high-T_c superconductors (HTSC's),[1] there has been a vigorous effort to determine their normal state electronic structure considered essential for an understanding of superconductivity in these materials. The prevailing opinion is that the electronic structure close to the Fermi level (E_F) is largely determined by the CuO_2 planes.

Recently, superconductivity below 0.93 K was observed in Sr_2RuO_4.[2] Despite the low T_c this material demands investigation as it is the first layered perovskite superconductor without Cu. Sr_2RuO_4 is isostructural to the high temperature phase of La_2CuO_4,[3] but contains RuO_2 planes. Thus, there is the opportunity to study the electronic structure of this compound and compare it to the HTSC's. As well as structural similarities, Sr_2RuO_4 displays some other properties seen in the cuprates; for example, the approximately linear temperature dependence of the in-plane resistivity down to 25 K (below 25 K the temperature dependence is quadratic). In a simple ionic picture the valence state of Ru is formally different to Cu. Copper is in a Cu^{2+} ($3d^9$) valence state with $S=1/2$, whereas Ru is assumed to be in a Ru^{4+} ($4d^4$) valence state with $S=1$, as suggested by studies of $Sr_2Ir_{1-x}Ru_xO_4$.[4] The tetragonal distortion of the RuO_6 octahedron will lead to a splitting of the t_{2g} and e_g levels. However, the Ru 4*d* orbitals are much more extended and more strongly hybridized than Cu 3*d*, leading to large ligand field splittings and larger band dispersions, as can be seen in a band-structure calculation for RuO_2.[5] While in La_2CuO_4 the t_{2g} levels are completely filled and the hole is in the antibonding Cu $3d_{x^2-y^2}$ orbitals, in Sr_2RuO_4 the t_{2g} levels are only partially filled. Information on the unoccupied states and their symmetry can be obtained by near-edge x-ray-absorption fine structure (NEXAFS) spectroscopy using polarized light. Furthermore, valence band photoemission spectroscopy (UPS) probes the occupied density of states, and may be compared to recent band-structure calculations.[6,7] Here we present NEXAFS and UPS experimental data on $Sr_2RuO_4(001)$ single crystals. The samples were platelike single crystalline Sr_2RuO_4 grown by a floating zone melting method.[8] The typical dimensions of the samples were $2\times1\times0.1$ mm^3. T_c measured on samples of the same batch was about 1 K.

Experiments were carried out in three separate laboratories. NEXAFS measurements were recorded in the total electron yield (TEY) mode at the 5U.1 undulator beamline at the Synchrotron Radiation Source, Daresbury Laboratory (SRS),[9,10] collecting the emitted electrons with a channeltron, and in the fluorescence yield (FY) mode at beamline U4B at the National Synchrotron Light Source (NSLS), with an ultra-low energy Ge detector. The resolution for the NEXAFS O 1*s* spectra taken at SRS was about 400 meV and at NSLS about 200 meV. The FY spectra were corrected for self-absorption effects.[11] Photoemission spectroscopy was performed at SRS using a VSW 100 mm hemispherical analyzer with an angular acceptance of $\pm4°$. The resolution used for UPS was about 200 meV and for x-ray photoemission spectroscopy (XPS) about 400 meV. Sample surfaces suitable for UPS, XPS and NEXAFS at SRS were prepared by *in situ* cleaving of $Sr_2RuO_4(001)$ crystals at 160 K using a tab technique in a vacuum better than 3×10^{-10} mbar. Just one hour after cleaving at this pressure, however, there were signs of contamination, which will be discussed later. No surface preparation is necessary for NEXAFS using the FY mode. Angle-resolved UPS (ARUPS) spectra of $Sr_2RuO_4(001)$ crystals were performed at Karlsruhe with a discharge lamp using the Ne I line at 16.85 eV (contributions from the satellite line at 16.67 eV were subtracted for the spectra shown). The angular acceptance of the hemispherical analyzer (VSW HA50) was $\pm1°$ and the energy resolution was 100 meV. The samples were oriented using Laue diffraction and then cleaved *in situ* at 10 K using a tab technique in a vacuum better than 3×10^{-11} mbar. Samples remained clean for about 12 hours. During the NEXAFS measurements we could not detect any changes due to contamination. This behavior reflects the larger sampling depth of TEY (50–100 Å) and FY (1500–3500 Å) in comparison to photoemission ($\approx$10 Å).

Figure 1 shows the O 1*s* x-ray-absorption spectra taken in FY and TEY mode of $Sr_2RuO_4(001)$ for three orientations of the sample surface towards the polarization vector. At $\theta_i=0°$ the light polarization is parallel to the RuO_2 plane; in this orientation electrons are excited from the O 1*s* core level, due to the dipole selection rule, only into unoccupied

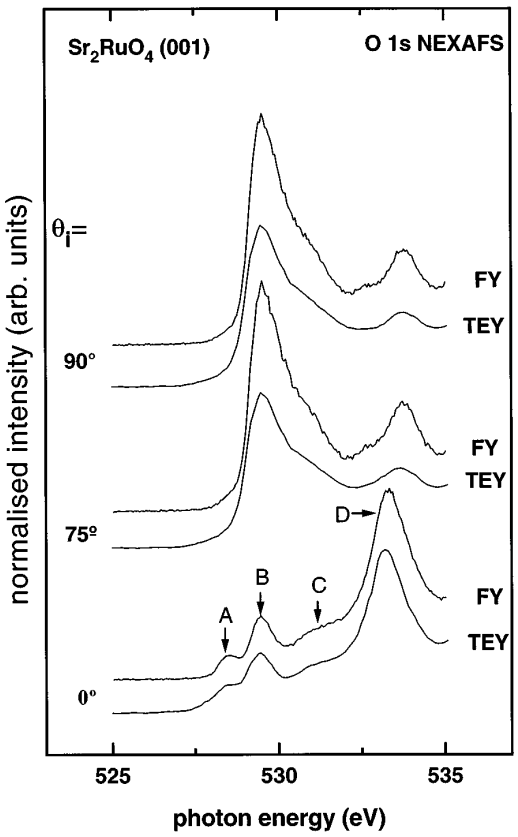

FIG. 1. O 1*s* NEXAFS of Sr_2RuO_4. The angle θ_i denotes the angle between the incident beam and the surface normal. The spectra labeled TEY are taken using the total electron yield method, while for the spectra labeled FY we used the fluorescence yield mode. The 90° spectrum was deduced from the 0° and 75° spectra. The peaks labeled *A* to *D* are discussed in the text.

O $2p_{x,y}$ orbitals. At an orientation of $\theta_i = 90°$ electrons are excited from the O 1*s* core level to unoccupied levels with O $2p_z$ symmetry. The 90° spectrum, which is experimentally not accessible, was deduced from the 0° and 75° spectra. The spectra obtained by these two methods are remarkably similar including relative peak heights within one orientation, indicating that there is a strong resemblance between the electronic structure of the surface region (TEY) and of the bulk (FY). One major difference is that the absolute height of the TEY spectra at $\theta_i = 75°$ and 90° is different to the FY spectra. This may be due to an extrinsic background in the TEY spectra, which is absent in the FY spectra. In the following, quantitative estimates are deduced from the FY spectra.

Let us consider the angular dependence of the spectra in Fig. 1. Feature *A* at a photon energy of 528.5 eV is very pronounced at $\theta_i = 0°$ in comparison to $\theta_i = 90°$. However, the spectral weight of this peak is very small in comparison to the other features. The spectral weight of feature *B* associated with the O 2*p* orbitals vertical to the plane (p_z) appears to be four times as high as the intensity of the orbitals in the plane ($p_{x,y}$), but there, for a given light polarization only half of the holes with p_x and p_y symmetry are detected. Thus, spectral weight perpendicular to the planes is, in fact, twice as large as in the plane. Feature *C* is not very pronounced and has nearly equal contributions in the plane and perpendicular to the plane, while feature *D* has an in-plane contribution twice as large as the out-of-plane contribution. According to a band-structure calculation for RuO_2,[5] the crystal field splitting between orbitals with t_{2g} and e_g symmetry is about 4 eV. This result and the observed spectral weight and angular dependence of the peaks *A*–*D* lead us to assign these peaks as follows: peaks *A* and *B* correspond to orbitals with t_{2g} symmetry and peaks *C* and *D* to orbitals with e_g symmetry. Peak *A* is related to the apical oxygen O(2) whose core level binding energy according to the band-structure calculation for Sr_2RuO_4 is 1.5 eV smaller than for the in-plane oxygen O(1).[6] An in-plane hybridization of O(2) holes with Ru $4d_{xz}$ and $4d_{yz}$ orbitals, which is according to the band-structure calculation very small, could explain the low intensity of feature *A* compared to feature *B*. We presume that E_F for O(1) corresponds to 529 eV. The large contribution of holes perpendicular to the planes for peak *B* is due to O(1) $2p\pi$ orbitals hybridized with Ru $4d_{xz}, 4d_{yz}$. The bands with Ru $4d_{xz}, 4d_{yz}$ character should cross E_F and are therefore the main contribution to peak *B* perpendicular to the plane. The in-plane contribution of feature *B* is caused by Ru $4d_{xy}$-O(1) $2p\pi$ orbitals. This assignment leads to the interesting conclusion that the number of holes in the Ru $4d_{xz,yz}$-O(1) $2p\pi$ bands is twice as large as in the Ru $4d_{xy}$-O(1) $2p\pi$ band. Peak *C* may be explained by Ru $4d\gamma$ ($4d_{3z^2-r^2}, 4d_{x^2-y^2}$) states hybridized with O $2p\sigma$ states, since it has an in-plane and an out-of-plane contribution. Spectral weight at higher photon energies is more difficult to assign to certain orbitals. The in-plane contribution of feature *D* is located at 533.3 eV, while the out-of-plane contribution is located at 533.8 eV, indicating that two different levels are involved. The in-plane contribution of feature *D* is caused by Ru $4d_{x^2-y^2}$ O(1) $2p\sigma$ states, while the out-of-plane level is caused by the Ru $4d_{3z^2-r^2}$-O(2) $2p\sigma$ states. However, SrO bands may contribute to feature *D* as well. Coulomb interaction between electrons and holes at the Ru sites is expected to be smaller than in the cuprates, while the bandwidth is larger. Thus a contribution from an upper Hubbard band, as observed in La_2CuO_4,[12,13] is unlikely for our spectra.

Figure 2(a) shows the angle integrated photoemission spectra at photon energies of 60 and 110 eV and the calculated density of states.[6] The spectra were obtained immediately after cleaving the sample. The total valence band width is around 9 eV, slightly larger than the calculated width. A Shirley background was subtracted to account for secondary electrons. A sharp peak at E_F is observed with a width of about 700 meV. However, since we cannot resolve individual bands, this is a poor estimate for the occupied part of the conduction bands. Peaks *A* and *B* are separated by an intensity valley 1.3 eV wide. According to the band-structure calculations[6,7] the states close to E_F are the occupied part of the antibonding Ru $4d\epsilon$ ($4d_{xy}, 4d_{xz}, 4d_{yz}$) and O $2p\pi$ orbitals. The width of feature *A* as well as the intensity valley are in qualitative agreement with the band-structure calculations,[6,7] although the intensity in the valley region is much lower in the calculations. Peak *A* at E_F is very intense for $h\nu = 60$ eV in comparison to $h\nu = 110$ eV. To obtain a quantitative value for the density of states at E_F, $N(E_F)$, we used the 60 eV spectra since there the photoionization cross

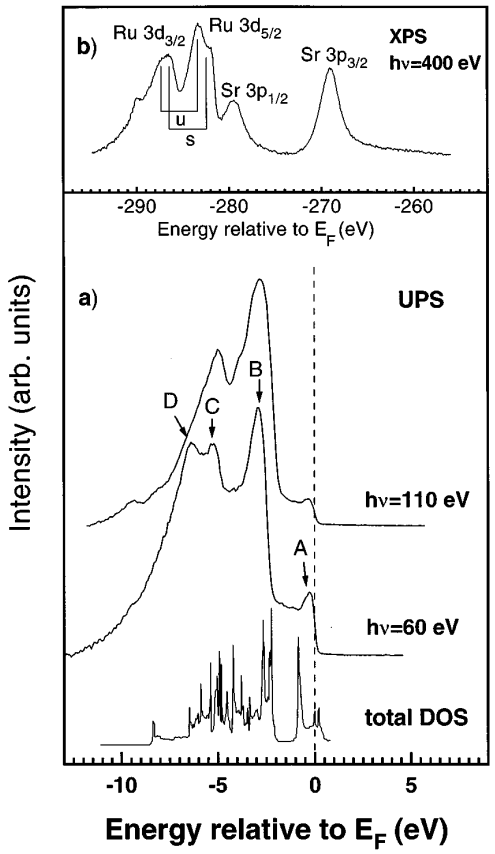

FIG. 2. (a) UPS data of the valence-band region of Sr_2RuO_4 recorded with a photon energy of 60 eV and 110 eV. The main structures are labeled *A* to *D*. The total density of states from the band-structure calculation of Singh (Ref. 6) is shown at the bottom. The upper panel (b) shows the XPS spectrum recorded with 400 eV photon energy in the Ru 3*d* and Sr 3*p* core level regions. The positions of screened (*s*) and unscreened (*u*) final states are indicated in the figure.

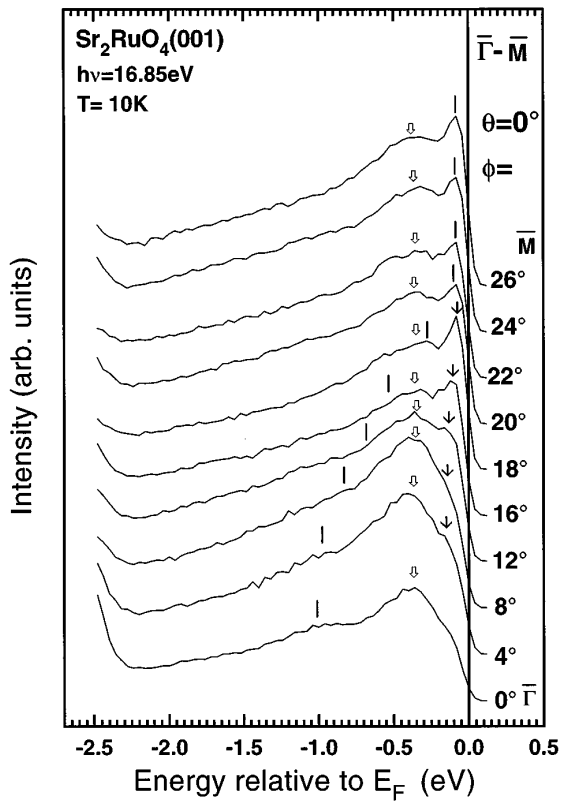

FIG. 3. ARUPS data of Sr_2RuO_4 along the $\bar{\Gamma}$-$\bar{M}$ line using Ne I radiation (contributions from the satellite line at 16.67 eV were subtracted for the spectra shown). Different symbols are assigned to peaks to denote individual bands as inspired by the band-structure calculation of Singh (Ref. 6).

sections of Ru 4*d* and O 2*p* are quite similar.[14] The relative ratio of the integrated area of feature *A* to the integrated area of the valence band is taken to be equivalent to the number of electrons at E_F divided by the total number of valence electrons, assuming the valence band is composed of Ru 4*d* and O 2*p* states. We arrive at $N(E_F)=1.4$ states/(eV cell). This value is a factor of 3 less than the prediction from band-structure calculation.[6] A corresponding $N(E_F)$ derived in a similar way by Arko *et al.* for $YBa_2Cu_3O_{7-\delta}$ is four times smaller than in Sr_2RuO_4.[15] We can also estimate the relative orbital contribution at E_F in a similar way to Arko *et al.* We arrive at 80% Ru 4*d* and 20% O 2*p* states at E_F. This is in contrast to the cuprates exhibiting 20% Cu and 80% O states at E_F.[15] Although our value is only a rough estimate since we neglected final state effects, it demonstrates that the states at E_F in Sr_2RuO_4 are mainly determined by Ru 4*d* electrons in agreement with the band-structure calculations.[6,7] While the features *B* and *C* do not show a large photon energy dependence, feature *D* is at least a factor of 2 lower in intensity at 110 eV. This may be either due to the reduced cross section of Ru 4*d* or due to a final state effect.

Figure 2(b) presents an XPS spectrum of the Ru 3*d* and Sr 3*p* core levels recorded with 400 eV photons. Each of the Ru $3d_{5/2}$ and Ru $3d_{3/2}$ core levels shows a splitting. This spectrum is very similar to the corresponding spectrum of $SrRuO_3$.[16] The splitting of the Ru 3*d* core levels may be explained within the model of Kotani and Toyazawa.[17] If the core-valence Coulomb interaction is larger than the conduction bandwidth, upon photoexcitation one of the valence orbitals will be disengaged from the conduction band. The resulting localized atomic state lies below E_F and may be filled with an electron. Two different final states correspond to the situation where this level is filled or unfilled, referred to as the screened and unscreened final states.

We should also note that the XPS spectrum was obtained three hours after cleaving and shows a shoulder at 290 eV binding energy, which is due to contamination of the sample surface. After another three hours this peak becomes even stronger with the rest of the spectrum nearly unchanged. Hence we are confident that the small contamination feature present in Fig. 2(b) does not affect our conclusions.

Direct information on the width of bands near E_F can be obtained by angle-resolved photoemission. ARUPS data shown in Fig. 3 are recorded along the $\bar{\Gamma}$-$\bar{M}$ direction in the projected Brillouin zone. The angles (θ,ϕ) displayed next to each energy distribution curve denote the emission direction of the collected photoelectrons towards the sample surface normal. High-resolution spectra, along the high symmetry lines for a very narrow energy range within E_F are presented elsewhere.[18] Band-structure calculations[6,7] predict three

bands to cross E_F and the bottom of these bands is at $\overline{\Gamma}$. Moving along $\overline{\Gamma}$-M we are able to observe these bands. We can identify a broad peak at around 1 eV below E_F at $\overline{\Gamma}$. Another peak at 0.4 eV is more pronounced. If we compare these two peaks with the band-structure calculation, we find that the bandwidth is renormalized by more than a factor of 2. The peak at 0.4 eV is composed of two features which become more clearly resolved as we move towards M. One band sharpens up and moves closer to E_F as we go towards the M point. A crossing could be observed at around 18° in agreement with our high resolution data.[18] We also observe a band staying at approximately 0.4 eV for the whole $\overline{\Gamma}$-M line. The dispersion of both bands is in qualitative agreement with the band-structure calculations.[6,7] The third band at 1 eV binding energy at $\overline{\Gamma}$ is dispersing towards E_F as we move closer to the M point. Although we are not able to resolve the dispersion of this band clearly, we believe by comparison with the band-structure calculation that this band moves towards E_F up until an angle of 22° at which point it remains at E_F up to M. This flat band leads to an extended van Hove singularity at the M point.[18] An angle-resolved photoemission study by Yokoya *et al.*[19] was not able to resolve all three bands close to E_F. Other UPS and XPS studies performed on a series of ternary ruthenium oxides including $SrRuO_3$ (Ref. 16) argued that the Ru 4*d* bandwidth is decreasing in the series $Pb_2Ru_2O_{7-y} > Bi_2Ru_2O_7 > SrRuO_3 > CaRuO_3 > Y_2Ru_2O_7$. In $Y_2Ru_2O_7$ the correlation energy U exceeds the one-electron bandwidth, leading to a non-metallic material with a localized t_{2g} configuration. Our result suggests that Sr_2RuO_4 is in a region where correlation effects are important, as can be seen by the narrowed bandwidth in comparison to band-structure calculations. However, it should be borne in mind that the valence bandwidth is still considerably larger than in the cuprates.

As already remarked above the surface of these crystals is very sensitive to contamination, which after several hours leads to extra peaks in the photoemission valence band spectrum. The most pronounced change is the filling of the gap-like structure close to E_F, leading to a broad peak at 1.5 eV binding energy. At the same time a peak at 9.5 eV appears and the peak at E_F vanishes. It should be noted that this broad peak at 1.5 eV, which is related to a contaminated surface, had previously been interpreted in terms of the precursor of the lower Hubbard band.[20]

In conclusion, we observe the unoccupied density of states close to E_F of Sr_2RuO_4 to be mainly determined by antibonding Ru $4d\epsilon$ and O $2p\pi$ orbitals. The holes close to E_F are mainly determined by the Ru $4d_{xz,yz}$-O $2p\pi$ orbitals. The states at higher energy are dominated by the antibonding Ru $4d\gamma$ and O $2p\sigma$ orbitals, in agreement with a Ru^{4+} valence and with band-structure calculations. The peak at E_F, as seen in the photoemission spectra, has an orbital composition of 80% Ru 4*d* and 20% O 2*p* in contrast to the cuprates where it is oxygen dominated. The density of states at E_F is higher than in the cuprates. The conduction bandwidth is reduced by more than a factor of 2 in comparison to the band-structure calculations. The narrowed bandwidth of the conduction bands shows that correlation effects are important in this compound.

We thank W. R. Flavell, A. G. Thomas, V. Chakarian, and Y. J. Idzerda for experimental support and D. Singh for providing us with his band-structure calculation. We also appreciate stimulating discussions with M. Merz. The help and support of the staff at SRS and NSLS was greatly appreciated, especially M. Roper, D. Teehan, and M. Surman. Funding for travel and time at SRS, Daresbury was provided by the European Large Scale Facility programme. The NSLS is part of Brookhaven National Laboratory, which is operated by the U.S. DOE.

[1] J. G. Bednorz and K. A. Müller, Z. Phys. B **64**, 188 (1986).
[2] Y. Maeno, H. Hashimoto, K. Yoshida, S. Nishizaki, T. Fujita, J. G. Bednorz, and F. Lichtenberg, Nature **372**, 532 (1994).
[3] T. Vogt and D. J. Buttrey, Phys. Rev. B **52**, 9843 (1995).
[4] R. J. Cava, B. Batlogg, K. Kiyono, H. Takagi, J. J. Krajewski, W. F. Peck, L. W. Rupp, and C. H. Chen, Phys. Rev. B **49**, 11 890 (1994).
[5] P. A. Cox, *Transition Metal Oxides* (Clarendon Press, Oxford, 1992), p. 70.
[6] D. J. Singh, Phys. Rev. B **52**, 1358 (1995).
[7] T. Oguchi, Phys. Rev. B **51**, 1385 (1995).
[8] F. Lichtenberg A. Catana, J. Mannhart, and D. G. Schlom, Appl. Phys. Lett. **60**, 1138 (1992).
[9] H. A. Padmore, Rev. Sci. Instrum. **60**, 1608 (1989).
[10] C. S. Mythen, G. van der Laan, and H. A. Padmore, Rev. Sci. Instrum. **63**, 1313 (1992).
[11] L. Tröger, D. Arvanitis, K. Baberschke, H. Michaelis, U. Grimm, and E. Zschech, Phys. Rev. B **46**, 3283 (1992).
[12] E. Pellegrin, N. Nücker, J. Fink, S. L. Molodtsov, A. Guttierez, E. Navas, O. Strebel, Z. Hu, M. Domke, G. Kaindl, S. Uchida, Y. Nakamura, J. Markl, M. Klauda, G. Saemann-Ischenko, A. Krol, J. L. Peng, Z. Y. Li, and R. L. Greene, Phys. Rev. B **47**, 3354 (1993).
[13] C. T. Chen, L. H. Tjeng, J. Kwo, H. L. Kao, P. Rudolf, F. Sette, and R. M. Flemming, Phys. Rev. Lett. **68**, 2543 (1992).
[14] J. J. Yeh and I. Lindau, At. Data Nucl. Data Tables **32**, 1 (1985).
[15] A. J. Arko, R. S. List, R. J. Bartlett, S.-W. Cheong, Z. Fisk, J. D. Thompson, C. G. Olson, A.-B. Yang, R. Liu, C. Gu, B. W. Veal, J. Z. Liu, A. P. Paulikas, K. Vandervoort, H. Claus, J. C. Campuzano, J. E. Schirber, and N. D. Shinn, Phys. Rev. B **40**, 2268 (1989).
[16] P. A. Cox, R. G. Egdell, J. B. Goodenough, A. Hamnett, and C. C. Naish, J. Phys. C **16**, 912 (1974).
[17] A. Kotani and Y. Toyazawa, J. Phys. Soc. Jpn. **37**, 912 (1974).
[18] D. H. Lu, M. Schmidt, T. R. Cummins, S. Schuppler, F. Lichtenberg, and J. G. Bednorz, Phys. Rev. Lett. (to be published).
[19] T. Yokoya, A. Chainaini, T. Takahashi, H. Katayama-Yoshida, M. Kasai, and Y. Tokura, J. Phys. Chem. Solids **56**, 1885 (1995).
[20] I. H. Inoue, Y. Aiura, Y. Nishihara, Y. Haruyama, S. Nishizaki, Y. Maeno, T. Fujita, J. G. Bednorz, and F. Lichtenberg (unpublished).